LETTER **Communicated by Jurgen Schmidhuber**

Continuous Online Sequence Learning with an Unsupervised Neural Network Model

Yuwei Cui
ycui@numenta.com
Subutai Ahmad
sahmad@numenta.com
Jeff Hawkins
jhawkins@numenta.com
Numenta, Inc. Redwood City, CA 94063, U.S.A.

The ability to recognize and predict temporal sequences of sensory inputs is vital for survival in natural environments. Based on many known properties of cortical neurons, hierarchical temporal memory (HTM) sequence memory recently has been proposed as a theoretical framework for sequence learning in the cortex. In this letter, we analyze properties of HTM sequence memory and apply it to sequence learning and prediction problems with streaming data. We show the model is able to continuously learn a large number of variable order temporal sequences using an unsupervised Hebbian-like learning rule. The sparse temporal codes formed by the model can robustly handle branching temporal sequences by maintaining multiple predictions until there is sufficient disambiguating evidence. We compare the HTM sequence memory with other sequence learning algorithms, including statistical methods—autoregressive integrated moving average; feedforward neural networks—time delay neural network and online sequential extreme learning machine; and recurrent neural networks—long short-term memory and echo-state networks on sequence prediction problems with both artificial and real-world data. The HTM model achieves comparable accuracy to other state-of-the-art algorithms. The model also exhibits properties that are critical for sequence learning, including continuous online learning, the ability to handle multiple predictions and branching sequences with high-order statistics, robustness to sensor noise and fault tolerance, and good performance without task-specific hyperparameter tuning. Therefore, the HTM sequence memory not only advances our understanding of how the brain may solve the sequence learning problem but is also applicable to real-world sequence learning problems from continuous data streams.

Neural Computation **28, 2474–2504** (2016)
doi:10.1162/NECO_a_00893

1 Introduction

In natural environments, the cortex continuously processes streams of sensory information and builds a rich spatio temporal model of the world. The ability to recognize and predict ordered temporal sequences is critical to almost every function of the brain, including speech recognition, active tactile perception, and natural vision. Neuroimaging studies have demonstrated that multiple cortical regions are involved in temporal sequence processing (Clegg, Digirolamo, & Keele, 1998; Mauk & Buonomano, 2004). Recent neurophysiology studies have shown that even neurons in primary visual cortex can learn to recognize and predict spatiotemporal sequences (Gavornik & Bear, 2014; Xu, Jiang, Poo, & Dan, 2012) and that neurons in primary visual and auditory cortex exhibit sequence sensitivity (Brosch & Schreiner, 2000; Nikolić, Häusler, Singer, & Maass, 2009). These studies suggest that sequence learning is an important problem that is solved by many cortical regions.

Machine learning researchers have also extensively studied sequence learning independent of neuroscience. Statistical models, such as hidden Markov models (HMM; Fine, Singer, & Tishby, 1998; Rabiner & Juang, 1986) and autoregressive integrated moving average (ARIMA; Durbin & Koopman, 2012), have been developed for temporal pattern recognition and time-series prediction, respectively. A variety of neural network models have been proposed to model sequential data. Feedforward networks such as time-delay neural networks (TDNN) have been used to model sequential data by adding a set of delays to the input (Waibel, Hanazawa, Hinton, Shikano, & Lang, 1989). Recurrent neural networks can model sequence structure with recurrent lateral connections and process the data sequentially one record at a time. For example, long short-term memory (LSTM) has the ability to selectively pass information across time and can model very long-term dependencies using gating mechanisms (Hochreiter & Schmidhuber, 1997) and gives impressive performance on a wide variety of real-world problems (Greff, Srivastava, Koutnik, Steunebrink, & Schmidhuber, 2015; Lipton, Berkowitz, & Elkan, 2015; Sutskever, Vinyals, & Le, 2014). Echo state network (ESN) uses a randomly connected recurrent network as a dynamics reservoir and models a sequence as a trainable linear combination of these response signals (Jaeger & Haas, 2004).

Can machine learning algorithms gain any insight from cortical algorithms? The current state-of-the-art statistical and machine learning algorithms achieve impressive prediction accuracy on benchmark problems However, most time-series prediction benchmarks do not focus on model performance in dynamic, nonstationary scenarios. Benchmarks typically have separate training and testing data sets, where the underlying assumption is that the test data share similar statistics as the training data (Ben Taieb, Bontempi, Atiya, & Sorjamaa, 2012; Crone, Hibon, & Nikolopoulos, 2011). In contrast, sequence learning in the brain has to occur continuously to deal

with the noisy, constantly changing streams of sensory inputs. Notably, with the increasing availability of streaming data, there is also an increasing demand for online sequence algorithms that can handle complex, noisy data streams. Therefore, reverse-engineering the computational principles used in the brain could offer additional insights into the sequence learning problem that lies at the heart of many machine learning applications.

The exact neural mechanisms underlying sequence memory in the brain remain unknown, but biologically plausible models based on spiking neurons have been studied. For example, Rao and Sejnowski (2001) showed that spike-time-dependent plasticity rules can lead to predictive sequence learning in recurrent neocortical circuits. Spiking recurrent network models have been shown to recognize and recall precisely timed sequences of inputs using supervised learning rules (Brea, Senn, & Pfister, 2013; Ponulak & Kasiński, 2010). These studies demonstrate that certain limited types of sequence learning can be solved with biologically plausible mechanisms. However, only a few practical sequence learning applications use spiking network models as these models recognize only relatively simple and limited types of sequences. These models also do not match the performance of nonbiological statistical and machine learning approaches on real-world problems.

In this letter, we present a comparative study of HTM sequence memory, a detailed model of sequence learning in the cortex (Hawkins & Ahmad, 2016). The HTM neuron model incorporates many recently discovered properties of pyramidal cells and active dendrites (Antic, Zhou, Moore, Short, & Ikonomu, 2010; Major, Larkum, & Schiller, 2013). Complex sequences are represented using sparse distributed temporal codes (Ahmad & Hawkins, 2016; Kanerva, 1988), and the network is trained using an online unsupervised Hebbian-style learning rule. The algorithms have been applied to many practical problems, including discrete and continuous sequence prediction, anomaly detection (Lavin & Ahmad, 2015), and sequence recognition and classification.

We compare HTM sequence memory with four popular statistical and machine learning techniques: ARIMA, a statistical method for time-series forecasting (Durbin & Koopman 2012); extreme learning machine (ELM), a feedforward network with sequential online learning (Huang, Zhu, & Siew, 2006; Liang, Huang, Saratchandran, & Sundararajan, 2006); and two recurrent networks, LSTM and ESN. We show that HTM sequence memory achieves comparable prediction accuracy to these other techniques. In addition, it exhibits a set of features that is desirable for real-world sequence learning from streaming data. We demonstrate that HTM networks learn complex high-order sequences from data streams, rapidly adapt to changing statistics in the data, naturally handle multiple predictions and branching sequences, and exhibit high tolerance to system faults.

The letter is organized as follows. In section 2, we discuss a list of desired properties of sequence learning algorithms for real-time streaming data

analysis. In section 3, we introduce the HTM temporal memory model. In sections 4 and 5, we apply the HTM temporal memory and other sequence learning algorithms to discrete artificial data and continuous real-world data, respectively. Discussion and conclusions are given in section 6.

2 Challenges of Real-Time Streaming Data Analysis

With the increasing availability of streaming data, the demand for online sequence learning algorithms is increasing. Here, a data stream is an ordered sequence of data records that must be processed in real time using limited computing and storage capabilities. In the field of data stream mining, the goal is to extract knowledge from continuous data streams such as computer network traffic, sensor data, and financial transactions (Domingos & Hulten, 2000; Gaber, Zaslavsky, & Krishnaswamy, 2005; Gama, 2010), which often have changing statistics (nonstationary) (Sayed-Mouchaweh & Lughofer, 2012). Real-world sequence learning from such complex, noisy data streams requires many other properties in addition to prediction accuracy. This stands in contrast to many machine learning algorithms, which are developed to optimize performance on static data sets and lack the flexibility to solve real-time streaming data analysis tasks.

In contrast to these algorithms, the cortex solves the sequence learning problem in a drastically different way. Rather than achieving optimal performance for a specific problem (e.g., through gradient-based optimization), the cortex learns continuously from noisy sensory input streams and quickly adapts to the changing statistics of the data. When information is insufficient or ambiguous, the cortex can make multiple plausible predictions given the available sensory information.

Real-time sequence learning from data streams presents unique challenges for machine learning algorithms. In addition to prediction accuracy, we list a set of criteria that apply to both biological systems and real-world streaming applications.

2.1 Continuous Learning. Continuous data streams often have changing statistics. As a result, the algorithm needs to continuously learn from the data streams and rapidly adapt to changes. This property is important for processing continuous real-time sensory streams but has not been well studied in machine learning. For real-time data stream analysis, it is valuable if the algorithm can recognize and learn new patterns rapidly.

Machine learning algorithms can be classified into batch or online learning algorithms. Both types of algorithms can be adopted for continuous learning applications. To apply a batch-learning algorithm to continuous data stream analysis, one needs to keep a buffered data set of past data records. The model is retrained at regular intervals because the statistics of the data can change over time. The batch-training paradigm potentially requires significant computing and storage resources, particularly in

situations where the data velocity is high. In contrast, online sequential algorithms can learn sequences in a single pass and do not require a buffered data set.

2.2 High-Order Predictions. Real-world sequences contain contextual dependencies that span multiple time steps (i.e., the ability to make high-order predictions). The term *order* refers to Markov order, specifically the minimum number of previous time steps the algorithm needs to consider in order to make accurate predictions. An ideal algorithm should learn the order automatically and efficiently.

2.3 Multiple Simultaneous Predictions. For a given temporal context, there could be multiple possible future outcomes. With real-world data, it is often insufficient to consider only the single best prediction when information is ambiguous. A good sequence learning algorithm should be able to make multiple predictions simultaneously and evaluate the likelihood of each prediction online. This requires the algorithm to output a distribution of possible future outcomes. This property is present in HMMs (Rabiner & Juang, 1986) and generative recurrent neural network models (Hochreiter & Schmidhuber, 1997), but not in other approaches like ARIMA, which are limited to maximum likelihood prediction.

2.4 Noise Robustness and Fault Tolerance. Real-world sequence learning deals with noisy data sources where sensor noise, data transmission errors, and inherent device limitations frequently result in inaccurate or missing data. A good sequence learning algorithm should exhibit robustness to noise in the inputs.

The algorithm should also be able to learn properly in the event of system faults such as loss of synapses and neurons in a neural network. The property of fault tolerance and robustness to failure, present in the brain, is important for the development of next-generation neuromorphic processors (Tran, Yanushkevich, Lyshevski, & Shmerko, 2011). Noise robustness and fault tolerance ensure flexibility and wide applicability of the algorithm to a wide variety of problems.

2.5 No Hyperparameter Tuning. Learning in the cortex is extremely robust for a wide range of problems. In contrast, most machine learning algorithms require optimizing a set of hyperparameters for each task. It typically involves searching through a manually specified subset of the hyperparameter space, guided by performance metrics on a cross-validation data set. Hyperparameter tuning presents a major challenge for applications that require a high degree of automation, like data stream mining. An ideal algorithm should have acceptable performance on a wide range of problems without any task-specific hyperparameter tuning.

Many of the existing machine learning techniques demonstrate these properties to various degrees. A truly flexible and powerful system for streaming analytics would meet all of them. In the rest of the letter, we compare HTM sequence memory with other common sequence learning algorithms (ARIMA, ELM, ESN, TDNN, and LSTM) on various tasks using the above criteria.

3 HTM Sequence Memory

In this section we describe the computational details of HTM sequence memory. We first describe our neuron model. We then describe the representation of high-order sequences, followed by a formal description of our learning rules. We point out some of the relevant neuroscience experimental evidence in our description. A detailed mapping to the biology can be found in Hawkins and Ahmad (2016).

3.1 HTM Neuron Model. The HTM neuron (see Figure 1B) implements nonlinear synaptic integration inspired by recent neuroscience findings regarding the function of cortical neurons and dendrites (Major et al., 2013; Spruston, 2008). Each neuron in the network contains two separate zones: a proximal zone containing a single dendritic segment and a distal zone containing a set of independent dendritic segments. Each segment maintains a set of synapses. The source of the synapses is different depending on the zone (see Figure 1B). Proximal synapses represent feedforward inputs into the layer, whereas distal synapses represent lateral connections within a layer and feedback connections from a higher region. In this letter, we consider only a single layer and ignore feedback connections.

Each distal dendritic segment contains a set of lateral synaptic connections from other neurons within the layer. A segment becomes active if the number of simultaneously active connections exceeds a threshold. An active segment does not cause the cell to fire but instead causes the cell to enter a depolarized state, which we call the predictive state. In this way, each segment detects a particular temporal context and makes predictions based on that context. Each neuron can be in one of three internal states: an active state, a predictive state, or a nonactive state. The output of the neuron is always binary: it is active or not.

This neuron model is inspired by a large number of recent experimental findings that suggest neurons do not perform a simple weighted sum of their inputs and fire based on that sum (Polsky, Mel, & Schiller, 2004; Smith, Smith, Branco, & Häusser, 2013) as in most neural network models (LeCun, Bengio, & Hinton, 2015; McFarland, Cui, & Butts, 2013; Schmidhuber, 2014). Instead, dendritic branches are active processing elements. The activation of several synapses within close spatial and temporal proximity on a dendritic branch can initiate a local NMDA spike, which then causes a significant and

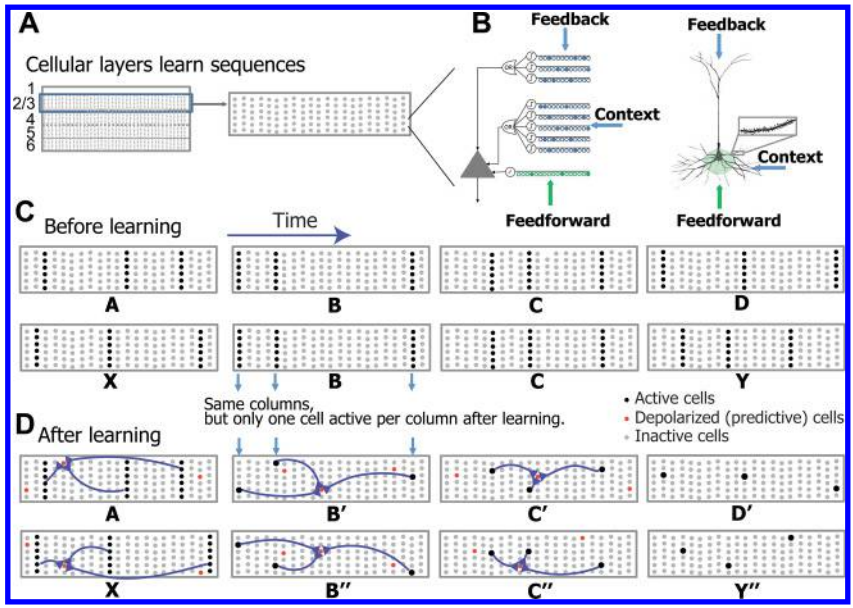

Figure 1: The HTM sequence memory model. (A) The cortex is organized into six cellular layers. Each cellular layer consists of a set of minicolumns, with each minicolumn containing multiple cells. (B) An HTM neuron (left) has three distinct dendritic integration zones, corresponding to different parts of the dendritic tree of pyramidal neurons (right). An HTM neuron models dendrites and NMDA spikes as an array of coincident detectors each with a set of synapses. The coactivation of a set of synapses on a distal dendrite will cause an NMDA spike and depolarize the soma (predicted state). (C, D) Learning high-order Markov sequences with shared sub-sequences (ABCD versus XBCY). Each sequence element invokes a sparse set of minicolumns due to intercolumn inhibition. (C) Prior to learning the sequences all the cells in a minicolumn become active. (D) After learning, cells that are depolarized through lateral connections become active faster and prevent other cells in the same column from firing through intracolumn inhibition. The model maintains two simultaneous representations: one at the minicolumn level representing the current feedforward input and the other at the individual cell level representing the context of the input. Because different cells respond to C in the two sequences (C′ and C″), they can invoke the correct high-order prediction of either D or Y.

sustained depolarization of the cell body (Antic et al., 2010; Major et al., 2013).

3.2 Two Separate Sparse Representations. The HTM network consists of a layer of HTM neurons organized into a set of columns (see Figure 1A). The network represents high-order sequences using a composition of two

separate sparse representations. At any time, both the current feedforward input and the previous sequence context are simultaneously represented using sparse distributed representations.

The first representation is at the column level. We assume that all neurons within a column detect identical feedforward input patterns on their proximal dendrites (Buxhoeveden, 2002; Mountcastle, 1997). Through an intercolumnar inhibition mechanism, each input element is encoded as a sparse distributed activation of columns at any point in time. At any time, the top 2% columns that receive the most active feedforward inputs are activated.

The second representation is at the level of individual cells within these columns. At any given time point, a subset of cells in the active columns will represent information regarding the learned temporal context of the current pattern. These cells in turn lead to predictions of the upcoming input through lateral projections to other cells within the same network. The predictive state of a cell controls inhibition within a column. If a column contains predicted cells and later receives sufficient feedforward input, these predicted cells become active and inhibit others within that column. If there were no cells in the predicted state, all cells within the column become active.

To illustrate the intuition behind these representations consider two abstract sequences A-B-C-D and X-B-C-Y (see Figures 1C and 1D). In this example remembering that the sequence started with A or X is required to make the correct prediction following C. The current inputs are represented by the subset of columns that contains active cells (black dots in Figures 1C and 1D). This set of active columns does not depend on temporal context, just on the current input. After learning, different cells in this subset of columns will be active depending on predications based on the past context (B′ versus B″, C′ versus C″, Figure 1D). These cells then lead to predictions of the element following C (D or Y) based on the set of cells containing lateral connections to columns representing C.

This dual representation paradigm leads to a number of interesting properties. First, the use of sparse representations allows the model to make multiple predictions simultaneously. For example, if we present input B to the network without any context, all cells in columns representing the B input will fire, which leads to a prediction of both C′ and C″. Second, because information is stored by coactivation of multiple cells in a distributed manner, the model is naturally robust to both noise in the input and system faults such as loss of neurons and synapses. (A detailed discussion on this topic can be found in Hawkins & Ahmad, 2016.)

3.3 HTM Activation and Learning Rules. The previous sections provided an intuitive description of network behavior. In this section we describe the formal activation and learning rules for the HTM network. Consider a network with N columns and M neurons per column; we denote the

activation state at time step t with an $M \times N$ binary matrix $\mathbf{A}^t$, where a_{ij}^t is the activation state of the ith cell in the jth column. Similarly, an $M \times N$ binary matrix Π^t denotes cells in a predictive state at time t, where π_{ij}^t is the predictive state of the ith cell in the jth column. We model each synapse with a scalar permanence value and consider a synapse connected if its permanence value is above a connection threshold. We use an $M \times N$ matrix $\mathbf{D}_{ij}^d$ to denote the permanence of the dth segment of the ith cell in the jth column. The synaptic permanence matrix is bounded between 0 and 1. We use a binary matrix $\tilde{D}_{ij}^d$ to denote only the connected synapses. The network can be initialized such that each segment contains a set of potential synapses (i.e., with nonzero permanence value) to a randomly chosen subset of cells in the layer. To speed up simulation, instead of explicitly initializing a complete set of synapses across every segment and every cell, we greedily create segments at run time (see the appendix).

The predictive state of the neuron is handled as follows: if a dendritic segment receives enough input, it becomes active and subsequently depolarizes the cell body without causing an immediate spike. Mathematically, the predictive state at time step t is calculated as follows:

$$\pi_{ij}^t = \begin{cases} 1 & \text{if } \exists_d \|\tilde{\mathbf{D}}_{ij}^d \circ \mathbf{A}^T\|_1 > \theta \\ 0 & \text{otherwise} \end{cases}. \tag{3.1}$$

Threshold θ represents the segment activation threshold, and $\circ$ represents element-wise multiplication. Since the distal synapses receive inputs from previously active cells in the same layer, it contains contextual information of past inputs, which can be used to accurately predict future inputs (see Figure 1B).

At any time, an intercolumnar inhibitory process selects a sparse set of columns that best match the current feedforward input pattern. We calculate the number of active proximal synapses for each column and activate the top 2% of the columns that receive the most synaptic inputs. We denote this set as $\mathbf{W}^t$. The proximal synapses were initialized such that each column is randomly connected to 50% of the inputs. Since we focus on sequence learning in this letter, the proximal synapses were fixed during learning. In principle, the proximal synapses can also adapt continuously during learning according to a spatial competitive learning rule (Hawkins, Ahmad, & Dubinsky, 2011; Mnatzaganian, Fokoué, & Kudithipudi, 2016).

Neurons in the predictive state (i.e., depolarized) will have competitive advantage over other neurons receiving the same feedforward inputs. Specifically, a depolarized cell fires faster than other nondepolarized cells if it subsequently receives sufficient feedforward input. By firing faster, it prevents neighboring cells in the same column from activating with intracolumn inhibition. The active state for each cell is calculated as follows:

$$a_{ij}^t = \begin{cases} 1 & \text{if } j \in \mathbf{W}^t \text{ and } \pi_{ij}^{t-1} = 1 \\ 1 & \text{if } j \in \mathbf{W}^t \text{ and } \sum_i \pi_{ij}^{t-1} = 0 \\ 0 & \text{otherwise} \end{cases}. \tag{3.2}$$

The first conditional expression of equation 3.2 represents a cell in a winning column becoming active if it was in a predictive state during the preceding time step. If none of the cells in a winning column are in a predictive state, all cells in that column become active, as in the second conditional of equation 3.2.

The lateral connections in the sequence memory model are learned using a Hebbian-like rule. Specifically, if a cell is depolarized and subsequently becomes active, we reinforce the dendritic segment that caused the depolarization. If no cell in an active column is predicted, we select the cell with the most activated segment and reinforce that segment. Reinforcement of a dendritic segment involves decreasing permanence values of inactive synapses by a small value p^- and increasing the permanence for active synapses by a larger value p^+:

$$\Delta \mathbf{D}_{ij}^d = p^+ \dot{\mathbf{D}}_{ij}^d \circ \mathbf{A}^{t-1} - p^- \dot{\mathbf{D}}_{ij}^d \circ (\mathbf{1} - \mathbf{A}^{t-1}). \tag{3.3}$$

$\dot{\mathbf{D}}_{ij}^d$ denotes a binary matrix containing only the positive entries in $\mathbf{D}_{ij}^d$, that is,

$$\dot{\mathbf{D}}_{ij}^d = \begin{cases} 1 \text{ if } \mathbf{D}_{ij}^d > 0 \\ 0 \text{ otherwise} \end{cases}. \tag{3.4}$$

We also apply a very small decay to active segments of cells that did not become active, mimicking the effect of long-term depression (Massey & Bashir, 2007):

$$\Delta \mathbf{D}_{ij}^d = p^{--} \dot{\mathbf{D}}_{ij}^d \text{ where } a_{ij}^t = 0 \text{ and } \|\tilde{\mathbf{D}}_{ij}^d \circ \mathbf{A}^{t-1}\|_1 > \theta, \tag{3.5}$$

where $p^{--} \ll p^-$.

The learning rule is inspired by neuroscience studies of activity-dependent synaptogenesis (Zito & Svoboda, 2002), which showed that the adult cortex generates new synapses in response to sensory activity rapidly. The mathematical formula we chose captured this Hebbian synaptogenesis learning rule. We did not derive the rule by implementing gradient descent on a cost function. There could be other mathematical formulations that give similar or better results.

A complete set of parameters and further implementation details can be found in the appendix. These parameters were set based on properties of sparse distributed representations (Ahmad & Hawkins, 2016). Notably, we

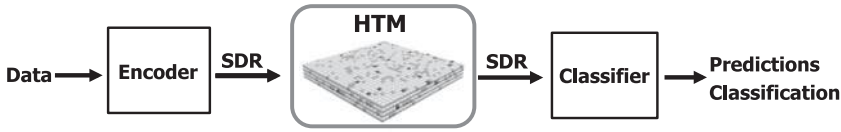

Figure 2: Functional steps for using HTM on real-world sequence learning tasks.

used the same set of parameters for all of the different types of sequence learning tasks in this letter.

3.4 SDR Encoder and Classifier. The HTM sequence memory operates with sparse distributed representations (SDRs) internally. To apply HTM to real-world sequence learning problems, we need to first convert the original data to SDRs using an encoder (see Figure 2). We have created a variety of encoders to deal with different data types (Purdy, 2016). In this letter, we used a random SDR encoder for categorical data and scalar and date-time encoders for the taxi passenger prediction experiment.

To decode prediction values from the output SDRs of HTM, we considered two classifiers: a simple classifier based on SDR overlaps and a maximum-likelihood classifier. For the single-step discrete sequence prediction task, we computed the overlap of the predicted cells with the SDRs of all observed elements and selected the one with the highest overlap. For the continuous scalar value prediction task, we divided the whole range of scalar value into 22 disjoint buckets and used a single-layer feedforward classification network. Given a large array of cell activation pattern $\mathbf{x}$, the classification network computes a probability distribution over all possible classes using a softmax activation function (Bridle, 1989). There are as many output units as the number of possible classes. The jth output unit receives a weighted summation of all the inputs,

$$a_j = \sum_{i=1}^{N} w_{ij} x_i. \tag{3.6}$$

w_{ij} is the connection weight from the ith input neuron to the jth output neuron. The estimated class probability is given by the activation level of the output units:

$$y_k = P\left(C_k|\mathbf{x}\right) = \frac{\mathbf{e}^{a_k}}{\sum_{i=1}^{K} \mathbf{e}^{a_k}}. \tag{3.7}$$

Using a maximum likelihood optimization, we derived the learning rule for the weight matrix $\mathbf{w}$:

$$\Delta w_{ij} = -\lambda(y_j - z_j)x_i. \tag{3.8}$$

z_j is the observed (target) distribution and λ is the learning rate. Note that since $\mathbf{x}$ is highly sparse, we only need to update a very small fraction of the weight matrix at any time. Therefore, the learning algorithm for the classifier is fast despite the high dimensionality of the weight matrix.

4 High-Order Sequence Prediction with Artificial Data

We conducted experiments to test whether the HTM sequence memory model, online sequential extreme learning machine (OS-ELM), time-delayed neural network (TDNN), and LSTM network are able to learn high-order sequences in an online manner, recover after modification to the sequences, and make multiple predictions simultaneously. LSTM represents the state-of-the-art recurrent neural network model for sequence learning tasks (Graves 2012; Hochreiter & Schmidhuber, 1997). OS-ELM is a feedforward neural network model that is widely used for time-series predictions (Huang, Wang, & Lan, 2011; Wang & Han, 2014). TDNN is a classical feedforward neural network designed to work with sequential data (Waibel et al., 1989). LSTM and HTM use the current pattern only as input and are able to learn the high-order structure. ELM and TDNN require the user to determine the number of steps to use as temporal context.

4.1 Continuous Online Learning from Streaming Data. We created a discrete high-order temporal sequence data set. Sequences are designed such that any learning algorithm would have to maintain context of at least the first two elements of each sequence in order to correctly predict the last element of the sequence (see Figure 3). We used the sequence data set in a continuous streaming scenario (see Figure 3C). At the beginning of a trial, we randomly chose a sequence from the data set and sequentially presented each of its elements. At the end of each sequence, we presented a single noise element to the model. The noise element is randomly chosen from a large set of 50,000 noise symbols (not used among the set of sequences). This is a difficult learning problem, since sequences are embedded in random noise; the start and end points are not marked. The set of noise symbols is large so the algorithm cannot learn every possible noise transition. We tested the algorithms for predicting the last element of each sequence continuously as the algorithm observed a stream of sequences and reported the percentage of correct predictions over time.

We encoded each symbol in the sequence as a random SDR for HTM sequence memory, with 40 randomly chosen active bits in a vector of 2048 bits. This SDR representation matches the internal representation used in HTM, which has 2048 columns with 40 active at any time (see the appendix). We initially tried to use the same SDR encoding for TDNN, ELM,

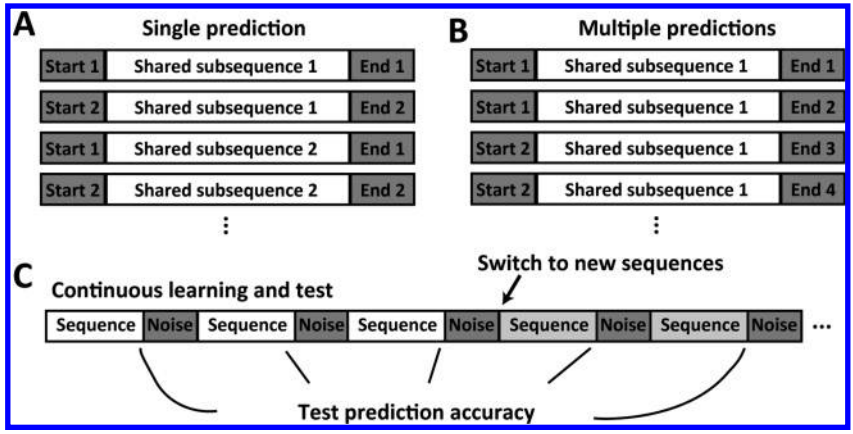

Figure 3: Design of the high-order sequence prediction task. (A). Structure of high-order sequences with shared sub-sequences. (B). High-order sequences with multiple possible endings. (C). Stream of sequences with noise between sequences. Both learning and testing occur continuously. After the model learned one set of sequences, we switched to a new set of sequences with contradictory endings to test the adaptation to changes in the data stream.

and LSTM. This high-dimensional representation does not work well due to the large number of parameters required. Instead, we used a random real-valued dense distributed representation for TDNN, ELM, and LSTM. Each symbol is encoded as a 25-dimensional vector with each dimension's value randomly chosen from $[-1, 1]$.[1] We chose this encoding format because it both gives better accuracy and has large representational capacity which is required for streaming data analysis. Similar dense distributed representations are commonly used for LSTM in natural language processing applications (Mikolov, Chen, Corrado, & Dean, 2013). We could not use one-hot vector encoding because its limited capacity prevents representing the noise elements between sequences, which are drawn from a very large dictionary.

Since the sequences are presented in a streaming fashion and predictions are required continuously, this task represents a continuous online learning problem. The HTM sequence memory is naturally suitable for online learning as it learns from every new data point and does not require the data stream to be broken up into predefined chunks. ELM also has a well-established online sequential learning model (Liang et al., 2006). An online sequential algorithm, such as real-time recurrent learning (RTRL), has been

[1]We manually tuned the number of dimensions and found that 25 dimensions gave the best performance on our tasks.

proposed for LSTM in the past (Hochreiter & Schmidhuber, 1997; Williams & Zipser, 1989). However, most LSTM applications used batch learning due to the high computational cost of RTRL (Jaeger, 2002). We use two variants of LSTM networks for this task. First, we retrained an LSTM network at regular intervals on a buffered data set of the previous time steps using a variant of the resilient backpropagation algorithm until convergence (Igel & Hüsken, 2003). The experiments include several LSTM models with varying buffer sizes. Second, we trained an LSTM network with online truncated backpropagation through time (BPTT) (Williams & Peng, 1990). At each time point, we calculated the gradient using BPTT over the last 100 elements and adjusted the parameters along the gradient by a small amount.

We tested sequences with either single or multiple possible endings (see Figures 3A and 3B). To quantify model performance, we classified the state of the model before presenting the last element of each sequence to retrieve the top K predictions, where $K = 1$ for the single prediction case and $K = 2$ or 4 for the multiple predictions case. We considered the prediction correct if the actual last element was among the top K predictions of the model. Since these are online learning tasks, there are no separate training and test phases. Instead, we continuously report the prediction accuracy of the end of each sequence before the model has seen it.

In the single prediction experiment (see Figure 4, left of the black solid line), each sequence in the data set has only one possible ending given its high-order context (see Figure 3A). The HTM sequence memory quickly achieves perfect prediction accuracy on this task (see Figure 4, red). Given a large enough learning window, LSTM also learns to predict the high-order sequences (see Figure 4, green). Despite comparable model performance, HTM and LSTM use the data in different ways: LSTM requires many passes over the learning window—each time it is retrained to perform gradient-descent optimization, whereas HTM needs to see each element only once (one-pass learning). LSTM also takes longer than HTM to achieve perfect accuracy; we speculate that since LSTM optimizes over all transitions in the data stream, including the random ones between sequences, it is initially overfitting on the training data. Online LSTM and ELM are also trained in an online, sequential fashion similar to HTM. But both algorithms require keeping a short history buffer of the past elements. ELM learned the sequences more slowly than HTM and never achieved perfect performance (see Figure 4, blue). Online LSTM has the best performance initially, but does not achieve perfect performance in the end. HTM, LSTM, and TDNN are able to achieve perfect prediction accuracy on this task.[2]

[2]For TDNN, the user has to know the length of temporal context ahead of time in order to obtain perfect performance. The results in Figure 3 used a lag of 10 steps. We could not obtain perfect performance with a lag of 5 or 20 steps.

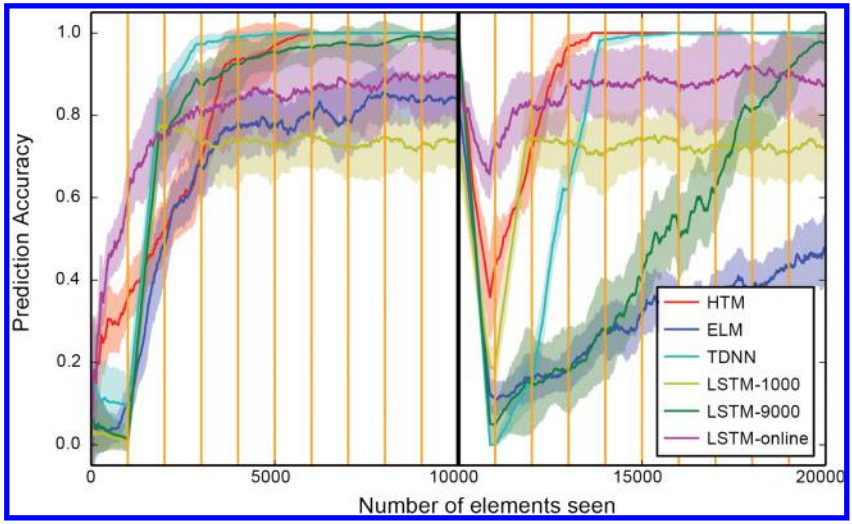

Figure 4: Prediction accuracy of HTM (red), LSTM (yellow, green, purple), ELM (blue), and TDNN (cyan) on an artificial data set. The data set contains four sixth order sequences and four seventh order sequences. Prediction accuracy is calculated as a moving average over the last 100 sequences. The sequences are changed after 10,000 elements have been seen (black dashed line). HTM sees each element once and learns continuously. ELM is trained continuously using a time lag of 10 steps. TDNN is retrained every 1000 elements (orange vertical lines) on the last 1000 elements (cyan). LSTM is either retrained every 1000 elements on the last 1000 elements (yellow) or 9000 elements (green), or continuously adapted using truncated BPTT (purple).

4.2 Adaptation to Changes in the Data Stream. Once the models have achieved stable performance, we altered the data set by swapping the last elements of pairs of high-order sequences (see Figure 4, black dashed line). This forces the model to forget the old sequences and subsequently learn the new ones. HTM sequence memory and online LSTM quickly recover from the modification. In contrast, it takes a long time for batch LSTM, TDNN, and ELM to recover from the modification as its buffered data set contains contradictory information before and after the modification. Although using a smaller learning window can speed up the recovery (see Figure 4, blue purple), it also causes worse prediction performance due to the limited number of training samples.

A summary of the model performance on the high-order sequence prediction task is shown in Figure 5. In general, there is a trade-off between prediction accuracy and flexibility. For batch learning algorithms, a shorter learning window is required for fast adaptation to changes in the data, but a longer learning window is required to perfectly learn high-order sequences

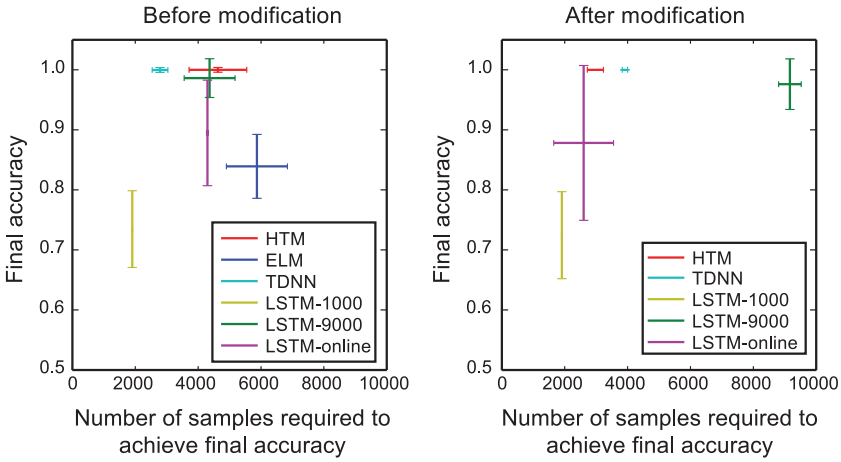

Figure 5: Final prediction accuracy as a function of the number of samples required to achieve final accuracy before (left) and after (right) modification of the sequences. Error bars represent standard deviations.

(see Figure 5, green versus yellow). Although online LSTM and ELM do not require batch learning, the user is required to specify the maximal lag, which limits the maximum sequence order it can learn. The HTM sequence memory model dynamically learns high-order sequences without requiring a learning window or a maximum sequence length. It achieved the best final prediction accuracy with a small number of data samples. After the modification to the sequences, HTM's recovery is much faster than ELM and LSTM trained with batch learning, demonstrating its ability to adapt quickly to changes in data streams.

4.3 Simultaneous Multiple Predictions. In the experiment with multiple predictions (see Figure 3B), each sequence in the data set has two or four possible endings, given its high-order context. The HTM sequence memory model rapidly achieves perfect prediction accuracy for both the 2-predictions and the 4-predictions cases (see Figure 6). While only these two cases are shown, in reality HTM is able to make many multiple predictions correctly if the data set requires it. Given a large learning window, LSTM is able to achieve good prediction accuracy for the 2-predictions case, but when the number of predictions is increased to 4 or greater, it is not able to make accurate predictions.

HTM sequence memory is able to simultaneously make multiple predictions due to its use of SDRs. Because there is little overlap between two random SDRs, it is possible to predict a union of many SDRs and classify a particular SDR as being a member of the union with low chance of a

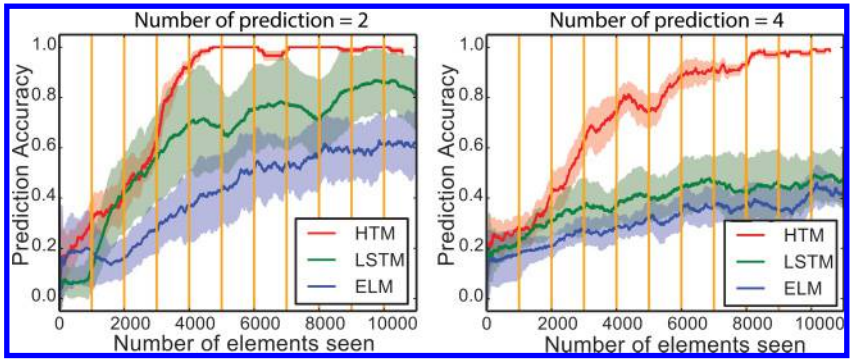

Figure 6: Performance on high-order sequence prediction tasks that require two (left) or four (right) simultaneous predictions. Shaded regions represent standard deviations (calculated with different sets of sequences). The data set contains four sets of sixth order sequences and four sets of seventh-order sequences.

false positive (Ahmad & Hawkins, 2016). On the other hand, the real-valued dense distributed encoding used in LSTM is not suitable for multiple predictions because the average of multiple dense representations in the encoding space is not necessarily close to any of the component encodings, especially when the number of predictions being made is large. The problem can be solved by using local one-hot representations to code target inputs, but such representations have very limited capacity and do not work well when the number of possible inputs is large or unknown upfront. This suggests that modifying LSTMs to use SDRs might enable better performance on this task.

4.4 Learning Long Term Dependencies from High-Order Sequences. For feedforward networks like ELM, the number of time lags that can be included in the input layer significantly limits the maximum sequence order a network can learn. The conventional recurrent neural networks cannot handle sequences with long-term dependencies because error signals "flowing backward in time" tend to either blow up or vanish with the classical backpropagation-through-time (BPTT) algorithm. LSTM is capable of learning very long-term dependencies using gating mechanisms (Henaff, Szlam, & Lecun, 2016). Here we tested whether HTM sequence memory can learn long-term dependencies by varying the Markov order of the sequences, which is determined by the length of shared sub-sequences (see Figure 3A).

We examined the prediction accuracy over training while HTM sequence memory learns variable-order sequences. The model is able to achieve perfect prediction performance up to 100-order sequences (see Figure 7A).

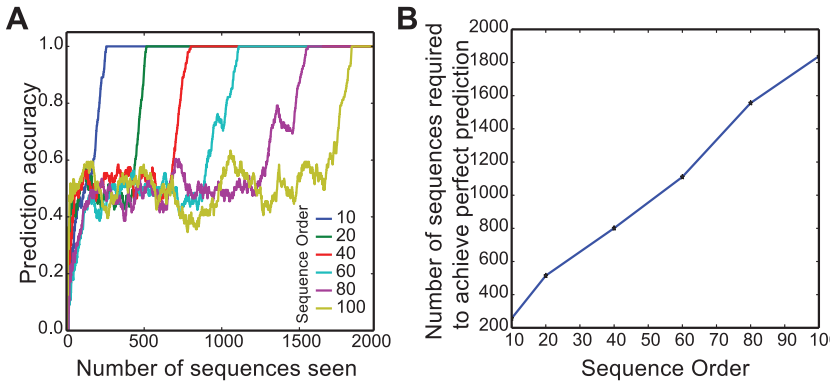

Figure 7: (A) Prediction accuracy over learning with sequences of different orders. (B) Number of sequences required to achieve perfect prediction as a function of sequence order. The sequence data set contains four high-order sequences with the structure shown in Figure 3A.

The number of sequences that are required to achieve perfect prediction performance increase linearly as a function of the order of sequences (see Figure 7B). Note that the model quickly achieves 50% accuracy much faster because it requires only first-order knowledge, yet it requires high-order knowledge to make a perfect prediction (see Figure 3A).

4.5 Disruption of High-Order Context with Temporal Noise. In the previous experiments, noise was presented between sequences. In this experiment, we tested the effect of noise within sequences. At run time, we randomly replaced either the second, third, or fourth element in each sequence with a random symbol. Such temporal noise could disrupt the high-order sequence context and make it much harder to predict the sequence endings. We considered two scenarios: (1) temporal noise throughout training and (2) noise introduced only after the models achieved perfect performance.

The performances of HTM and LSTM are shown in Figure 8. If temporal noise is present throughout training, neither HTM nor LSTM can make perfect predictions (see Figure 8A). LSTM has slightly better performance than HTM in this scenario, presumably because the gating mechanisms in LSTM can maintain some of the high-order sequence context. HTM behaves like a first-order model and has an accuracy of about 0.5. This experiment demonstrates the sensitivity of the HTM model to temporal noise.

If we inject temporal noise after the models achieve perfect performance on the noise-free sequences, the performance of both models drops rapidly (see Figure 8B). The performance of HTM drops to 0.5 (performance of the first-order model), whereas LSTM has worse performance. This result demonstrates that if the high-order sequence context is disrupted, HTM

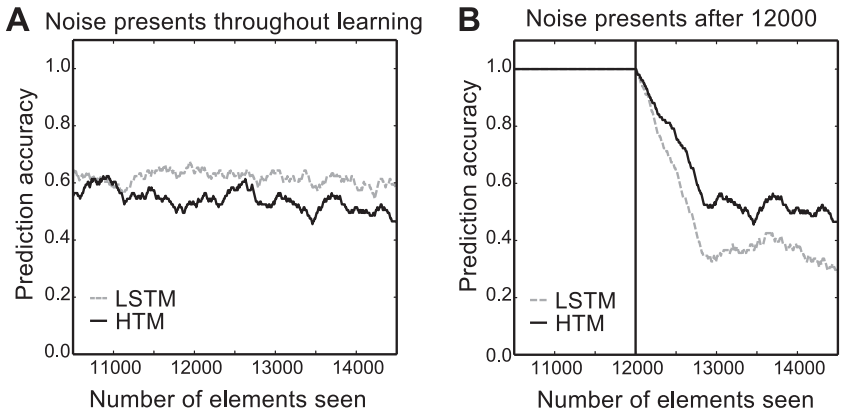

Figure 8: (A) Prediction accuracy over learning with the presence of temporal noise for LSTM (gray) and HTM (black). (B) HTM and LSTM are trained with clean sequences. Temporal noise was added after 12,000 elements. The sequence data set is same as in Figure 4.

would robustly behave as a low-order model, whereas the performance of LSTM is dependent on the training history.

4.6 Robustness of the Network to Damage. We tested the robustness of the ELM, LSTM, and HTM networks with respect to the removal of neurons. This fault tolerance property is important for hardware implementations of neural network models. After the models achieved stable performance on the high-order sequence prediction task (at the black dashed line, in Figure 2), we eliminated a fraction of the cells and their associated synaptic connections from the network. We then measured the prediction accuracy of both networks on the same data streams for an additional 5000 steps without further learning. There is no impact on the HTM sequence memory model performance at up to 30% cell death, whereas the performance of the ELM and LSTM networks declined rapidly with a small fraction of cell death (see Figure 9).

Fault tolerance of traditional artificial neural networks depends on many factors, such as the network size and training methods (Lee, Hwang, & Sung, 2014). The experiments here applied commonly used training methods for ELM and LSTM (see the appendix). It is possible that the fault tolerance of LSTM or any other artificial neural network may be improved by introducing redundancy (replicating trained network) (Tchernev, Mulvaney, & Phatak, 2005) or by a special training method such as dropout (Hinton, Krizhevsky, Sutskever, & Salakhutdinov, 2012). In contrast, the fault tolerance of HTM is naturally derived from properties of sparse

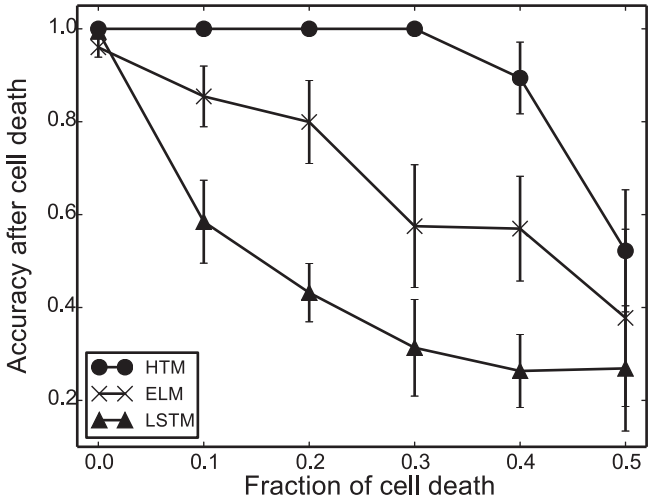

Figure 9: Robustness of the network to damage. The prediction accuracy after cell death is shown as a function of the fraction of cells that were removed from the network.

distributed representations (Ahmad & Hawkins, 2016), in analogy to biological neural networks.

5 Prediction of New York City Taxi Passenger Demand

In order to compare the performance of HTM sequence memory with other sequence learning techniques in real-world scenarios, we consider the problem of predicting taxi passenger demand. Specifically, we aggregated the passenger counts in New York City taxi rides at 30 minute intervals using a public data stream provided by the New York City Transportation Authority.[3] This leads to sequences exhibiting rich patterns at different timescales (see Figure 10A). The task is to predict taxi passenger demand five steps (2.5 hours) in advance. This problem is an example of a large class of sequence learning problems that require rapid processing of streaming data to deliver information for real-time decision making (Moreira-Matias, Gama, Ferreira, Mendes-Moreira, & Damas, 2013).

We applied HTM sequence memory and other sequence prediction algorithms to this problem. The ARIMA model is a widely used statistical approach for time series analysis (Hyndman & Athanasopoulos, 2013). As before, we converted ARIMA, TDNN, and LSTM to an online learning algorithm by retraining the models on every week of data with a buffered

[3]http://www.nyc.gov/html/tlc/html/about/trip_record_data.shtml.

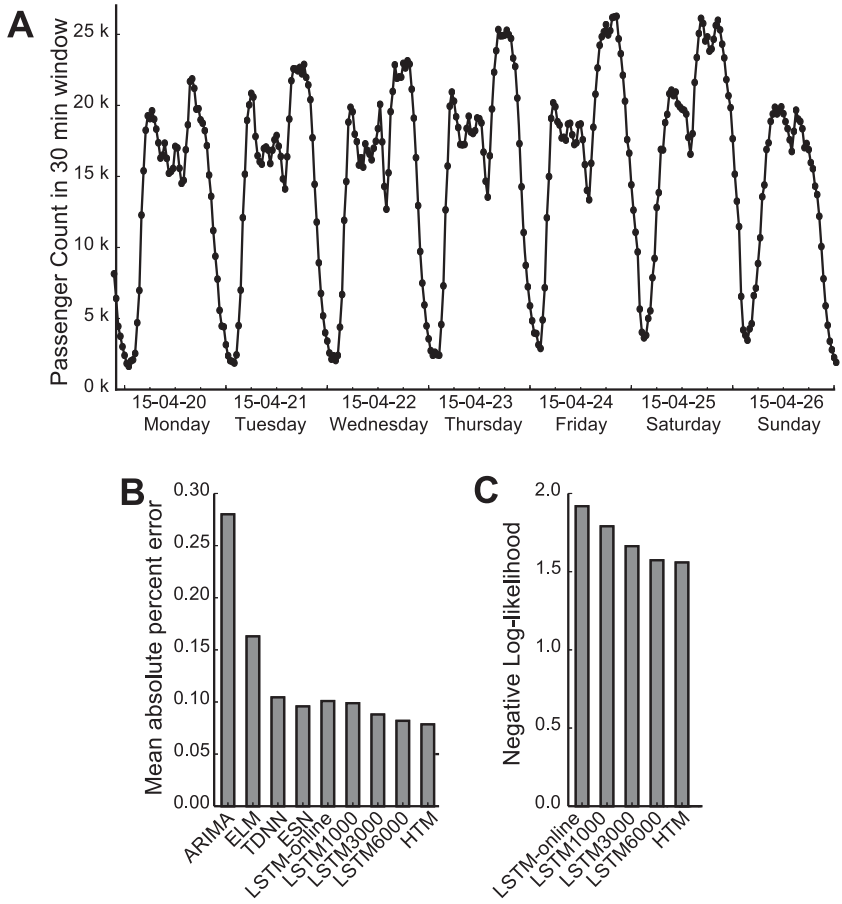

Figure 10: Prediction of the New York City taxi passenger data. (A) Example portion of taxi passenger data (aggregated at 30 min intervals). The data have rich temporal patterns at both daily and weekly timescales. (B, C) Prediction error of different sequence prediction algorithms using two metrics: mean absolute percentage error (B), and negative log likelihood (C).

data set of the previous 1000, 3000 or 6000 samples (see the appendix). ELM and ESN were adapted at every time step using sequential online learning methods. The parameters of the ESN, ELM, and LSTM network were extensively hand-tuned to provide the best possible accuracy on this data set The ARIMA model was optimized using R's "auto ARIMA" package (Hyndman & Khandakar, 2008). The HTM model did not undergo any parameter tuning; it uses the same parameters that were used for the previous artificial sequence task.

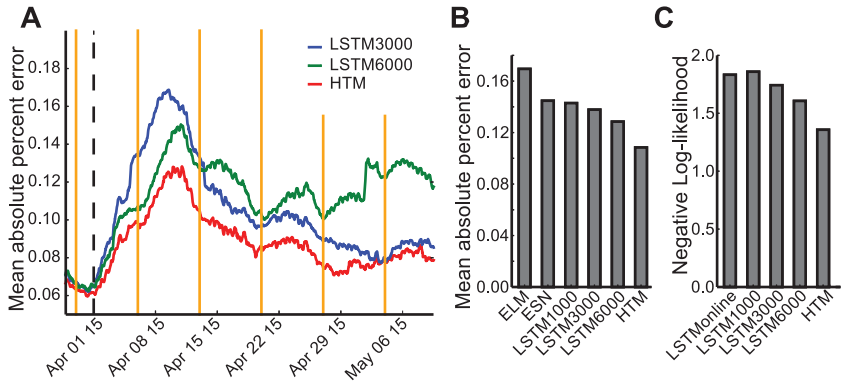

Figure 11: Prediction accuracy of LSTM and HTM after the introduction of new patterns. (A). The mean absolute percent error of HTM sequence memory (red) and LSTM networks (green, blue) after artificial manipulation of the data (black dashed line). The LSTM networks are retrained every week at the yellow vertical lines (B, C). Prediction error after the manipulation. HTM sequence memory has better accuracy on both the MAPE and the negative log-likelihood metrics.

We used two error metrics to evaluate model performance: mean absolute percentage error (MAPE) and negative log likelihood. The MAPE metrics focus on the single best point estimation, while negative log likelihood evaluates the models' predicted probability distributions of future inputs (see appendix for details). We found that the HTM sequence memory had comparable performance to LSTM on both error metrics. Both techniques had a much lower error than ELM, ESN, and ARIMA (see Figure 10B). Note that HTM sequence memory achieves this performance with a single-pass training paradigm, whereas LSTM requires multiple passes on a buffered data set.

We then tested how fast different sequence learning algorithms can adapt to changes in the data (see Figure 11). We artificially modified the data by decreasing weekday morning traffic (7 a.m.–11 a.m.) by 20% and increasing weekday night traffic (9 p.m.–11 p.m.) by 20% starting from April 1, 2015. These changes in the data caused an immediate increase in prediction error for both HTM and LSTM (see Figure 11A). The prediction error of HTM sequence memory quickly dropped back in about two weeks, whereas the LSTM prediction error stayed high much longer. As a result, HTM sequence memory had better prediction accuracy than LSTM and other models after the data modification (see Figures 11B and 11C).

6 Discussion and Conclusions

In this letter, we have applied HTM sequence memory, a recently developed neural network model, to real-time sequence learning problems with

time-varying input streams. The sequence memory model is derived from computational principles of cortical pyramidal neurons (Hawkins & Ahmad, 2016). We discussed model performance on both artificially generated and real-world data sets. The model satisfies a set of properties that are important for online sequence learning from noisy data streams with continuously changing statistics, a problem the cortex has to solve in natural environments. These properties govern the overall flexibility of an algorithm and its ability to be used in an automated fashion. Although HTM is still at a very early stage compared to other traditional neural network models, it satisfies these properties and shows promising results on real-time sequence learning problems.

6.1 Continuous Learning with Streaming Data. Most supervised sequence learning algorithms use a batch-training paradigm, where a cost function, such as prediction error, is minimized on a batch training data set (Bishop, 2006; Dietterich, 2002). Although we can train these algorithms continuously using a sliding window (Sejnowski & Rosenberg, 1987), this batch-training paradigm is not a good match for time-series prediction on continuous streaming data. A small window may not contain enough training samples for learning complex sequences, while a large window introduces a limit on how fast the algorithm can adapt to changing statistics in the data. In either case, a buffer must be maintained, and the algorithm must make multiple passes for every retraining step. It may be possible to use a smooth forgetting mechanism instead of hard retraining (Lughofer & Angelov, 2011; Williams & Zipser, 1989), but this requires the user to tune parameters governing the forgetting speed to achieve good performance.

In contrast, HTM sequence memory adopts a continuous learning paradigm. The model does not need to store a batch of data as the "training dataset." Instead, it learns from each data point using unsupervised Hebbian-like associative learning mechanisms (Hebb, 1949). As a result, the model rapidly adapts to changing statistics in the data.

6.2 Using Sparse Distributed Representations for Sequence Learning. A key difference between HTM sequence memory and previous biologically inspired sequence learning models (Abeles, 1982; Brea et al., 2013; Ponulak & Kasiński, 2010; Rao & Sejnowski, 2001) is the use of sparse distributed representations (SDRs). In the cortex, information is primarily represented by strong activation of a small set of neurons at any time, known as sparse coding (Földiák 2002, Olshausen & Field, 2004). HTM sequence memory uses SDRs to represent temporal sequences. Based on mathematical properties of SDRs (Ahmad & Hawkins, 2016; Kanerva, 1988), each neuron in the HTM sequence memory model can robustly learn and classify a large number of patterns under noisy conditions (Hawkins & Ahmad, 2016). A rich distributed neural representation for temporal sequences emerges from computation in HTM sequence memory. Although we focus on sequence prediction in this letter, this representation is valuable for a number

of tasks, such as anomaly detection (Lavin & Ahmad, 2015) and sequence classification.

The use of a flexible coding scheme is particularly important for online streaming data analysis, where the number of unique symbols is often not known upfront. It is desirable to be able to change the range of the coding scheme at run time without affecting previous learning. This requires the algorithm to use a flexible coding scheme that can represent a large number of unique symbols or a wide range of data. The SDRs used in HTM have a very large coding capacity and allow simultaneous representations of multiple predictions with minimal collisions These properties make SDR an ideal coding format for the next generation of neural network models.

6.3 Robustness and Generalization. An intelligent learning algorithm should be able to automatically deal with a large variety of problems without parameter tuning, yet most machine learning algorithms require a task-specific parameter search when applied to a novel problem. Learning in the cortex does not require an external tuning mechanism, and the same cortical region can be used for different functional purposes if the sensory input changes (Sadato et al., 1996; Sharma, Angelucci, & Sur, 2000). Using computational principles derived from the cortex, we show that HTM sequence memory achieves performance comparable to LSTM networks on very different problems using the same set of parameters. These parameters were chosen according to known properties of real cortical neurons (Hawkins & Ahmad, 2016) and basic properties of sparse distributed representations (Ahmad & Hawkins, 2016).

6.4 Limitations of HTM and Future Directions. We have identified a few limitations of HTM. First, as a strict one-pass algorithm with access to only the current input, it may take longer for HTM to learn sequences with very long-term dependencies (see Figure 7) than algorithms that have access to a longer history buffer. Learning of sequences with long-term dependencies can be sped up if we maintain a history buffer and run HTM on it multiple times. Indeed, it has been argued that an intelligent agent should store the entire raw history of sensory inputs and motor actions during interaction with the world (Schmidhuber, 2009). Although it may be computationally challenging to store the entire history, doing so may improve performance given the same amount of sensory experience.

Second, although HTM is robust to spatial noise due to the use of sparse distributed representations, the current HTM sequence memory model is sensitive to temporal noise. It can lose high-order sequence context if elements in the sequence are replaced by a random symbol (see Figure 8). In contrast, the gating mechanisms of LSTM networks appear to be more robust to temporal noise. The noise robustness of HTM can be improved by using a hierarchy of sequence memory models that operate on different timescales. A sequence memory model that operates over longer timescales

would be less sensitive to temporal noise. A lower region in the hierarchy may inherit the robustness to temporal noise through feedback connections to a higher region.

Third, the HTM model as discussed does not perform as well as LSTM on grammar learning tasks. We found that on the Reber grammar task (Hochreiter & Schmidhuber, 1997), HTM achieves an accuracy of 98.4% and ELM an accuracy of 86.7% (online training after observing 500 sequences), whereas LSTM achieves an accuracy of 100%. HTM can approximately learn artificial grammars by memorizing example sentences. This strategy could require more training samples to fully learn recursive grammars with arbitrary sequence lengths. In contrast, LSTM learns grammars much faster using the gating mechanisms. Unlike the HTM model, LSTMs can also model some Boolean algebra problems like the parity problem.

Finally, we have tested HTM only on low-dimensional categorical or scalar data streams in this letter. It remains to be determined whether HTM can handle high-dimensional data such as speech and video streams. The high capacity of the sparse distributed representations in HTM should be able to represent high-dimensional data. However, it is more challenging to learn sequence structure in high-dimensional space, as the raw data could be much less repeatable. It may require additional preprocessing, such as dimensionality reduction and feature extractions, before HTM can learn meaningful sequences with high-dimensional data. It would be an interesting future direction to explore how to combine HTM with other machine learning methods, such as deep networks, to solve high-dimensional sequence learning problems.

Appendix: Implementation Details

A.1 HTM Sequence Model Implementation Details. In our software implementation, we made a few simplifying assumptions to speed up simulation for large networks. We did not explicitly initialize a complete set of synapses across every segment and every cell. Instead, we greedily created segments on the least-used cells in an unpredicted column and initialized potential synapses on that segment by sampling from previously active cells. This happened only when there is no match to any existing segment. The initial synaptic permanence for newly created synapses is set as 0.21 (see Table 1), which is below the connection threshold (0.5).

The HTM sequence model operates with sparse distributed representations (SDRs). Specialized encoders are required to encode real-world data into SDRs. For the artificial data sets with categorical elements, we simply encoded each symbol in the sequence as a random SDR, with 40 randomly chosen active bits in a vector of 2048 bits.

For the New York City taxi data set, three pieces of information were fed into the HTM model: raw passenger count, the time of day, and the day of week (LSTM received the same information as input). We used NuPIC's

Table 1: Model Parameters for HTM.

Parameter Name	Value
Number of columns N	2048
Number of cells per column M	32
Dendritic segment activation threshold θ	15
Initial synaptic permanence	0.21
Connection threshold for synaptic permanence	0.5
Synaptic permanence increment p^+	0.1
Synaptic permanence decrement p^-	0.1
Synaptic permanence decrement for predicted inactive segments p^-	0.01
Maximum number of segments per cell	128
Maximum number of synapses per segments	128
Maximum number new synapses added at each step	32

standard scalar encoder to convert each piece of information into an SDR. The encoder converts a scalar value into a large binary vector with a small number of ON bits clustered within a sliding window, where the center position of the window corresponds to the data value. We subsequently combined three SDRs via a competitive sparse spatial pooling process, which also resulted in 40 active bits in a vector of 2048 bits as in the artificial data set. The spatial pooling process is described in detail in Hawkins et al. (2011).

The HTM sequence memory model used an identical set of model parameters for all the experiments described in the letter. A complete list of model parameters is shown below. The full source code for the implementation is available on Github at https://github.com/numenta/nupic.research.

A.2 Implementation Details of Other Sequence Learning Algorithms.

A.2.1 ELM. We used the online sequential learning algorithm for ELM (Liang et al., 2006). The network used 50 hidden neurons and a time lag of 100 for the taxi data and 200 hidden neurons and a time lag of 10 for the artificial data set.

A.2.2 ESN. We used the Matlab toolbox for echo state network developed by Jaeger's group (http://reservoir-computing.org/node/129). The ESN network has 100 internal units, a spectral radius of 0.1, a teacher scaling of 0.01, and a learning rate of 0.1 for the ESN model. The parameters were hand-tuned to achieve the best performance. We used the online learning mode and adapted the weight at every time step.

A.2.3 LSTM. We used the PyBrain implementation of LSTM (Schaul et al., 2010). For the artificial sequence learning task, the network contains 25 input units, 20 internal LSTM neurons, and 25 output units. For the NYC taxi task, the network contains 3 input units, 20 LSTM cells, 1 output unit

for calculation of the MAPE metric, and 22 output units for calculation of the sequence likelihood metric. The LSTM cells have forget gates but not peephole connections. The output units have a biased term. The maximum time lag is the same as the buffer size for the batch-learning LSTMs. We used two training paradigms. For the batch-learning paradigm, the networks were retrained every 1000 iterations with a popular version of the resilient backpropagation method (Igel & Hüsken 2003). For the online learning paradigm, we calculated the gradient at every time step using truncated backpropgation through time over the last 100 elements (Williams & Peng, 1990), and adjusted the parameters along the gradient with a learning rate of 0.01.

A.2.4 TDNN. Time-delayed neural network was implemented as a single hidden layer feedforward neural network with time-delayed inputs with PyBrain. For the artificial data set, the network contains 250 input units (10 time lags $\times$ 25 dimensional input per time step), 200 hidden units, and 25 output units. For the taxi data, the network contains 100 input units (100 time labs), 200 hidden units, and 1 output unit. We included bias for both input and output units in both cases. The networks were retrained every 1000 iterations (artificial data set) or every 336 iterations (taxi data) on the past 3000 data records using standard backpropagation.

A.3 Evaluation of Model Performance in the Continuous Sequence Learning Task. Two error metrics were used to evaluate the prediction accuracy of the model. First, we considered the mean absolute percentage error (MAPE) metric, an error metric that is less sensitive to outliers than root mean squared error:

$$\text{MAPE} = \frac{\sum_{t=1}^{N} |y_t - \hat{y}_t|}{\sum_{t=1}^{N} |y_t|}. \tag{A.1}$$

In equation A.1, y_t is the observed data at time t, $\hat{y}_t$ is the model prediction for the data observed at time t, and N is the length of the data set.

A good prediction algorithm should output a probability distribution of future elements of the sequence. However, MAPE, consider only the single best prediction from the model and thus does not incorporate other possible predictions from the model. We used negative log likelihood as a complementary error metric to address this problem. The sequence probability can be decomposed into

$$p(y_1, y_2, \ldots, y_t) = p(y_1)p(y_2|y_1)p(y_3|y_1, y_2)p(y_t|y_1, \ldots, y_{t-1}). \tag{A.2}$$

The conditional probability distribution is modeled by HTM or LSTM based on network state at the previous time step:

$$p(y_t|y_1, \ldots, y_{t-1}) = P(y_t|\text{network state}_{t-1}). \tag{A.3}$$

The negative log likelihood of the sequence is then given by

$$NLL = \frac{1}{N}\sum_{t=1}^{N} \log P(y_t|\text{model}). \tag{A.4}$$

Acknowledgments

We thank the NuPIC open source community (numenta.org) for continuous support and enthusiasm about HTM. We thank the reviewers for numerous suggestions that significantly improved the overall letter. We also thank Chetan Surpur for helping to run some of the simulations and our Numenta colleagues for many helpful discussions.

References

Abeles, M. (1982). *Local cortical circuits: An electrophysiological study*. Berlin: Springer.

Ahmad, S., & Hawkins, J. (2016). *How do neurons operate on sparse distributed representations? A mathematical theory of sparsity, neurons and active dendrites.* arXiv.1601.00720

Antic, S. D., Zhou, W. L., Moore, A. R., Short, S. M., & Ikonomu, K. D. (2010). The decade of the dendritic NMDA spike. *J. Neurosci. Res.*, *88*, 2991–3001.

Ben Taieb, S., Bontempi, G., Atiya, A. F., & Sorjamaa, A. (2012). A review and comparison of strategies for multi-step ahead time series forecasting based on the NN5 forecasting competition. *Expert Syst. Appl.*, *39*(8), 7067–7083.

Bishop, C. (2006). *Pattern recognition and machine learning*. Singapore: Springer.

Brea, J., Senn, W., & Pfister, J.-P. (2013). Matching recall and storage in sequence learning with spiking neural networks. *J. Neurosci.*, *33*(23), 9565–9575.

Bridle, J. (1989). Probabilistic interpretation of feedforward classification network outputs, with relationships to statistical pattern recognition. In F. Fogelman Soulié & J. Héravlt (Eds.), *Neurocomputing: Algorithms, architectures and applications* (pp. 227–236). Berlin: Springer-Verlag.

Brosch, M., & Schreiner, C. E. (2000). Sequence sensitivity of neurons in cat primary auditory cortex. *Cereb. Cortex.*, *10*(12), 1155–1167.

Buxhoeveden, D. P. (2002). The minicolumn hypothesis in neuroscience. *Brain*, *125*(5), 935–951.

Clegg, B. A., Digirolamo, G. J., & Keele, S. W. (1998). Sequence learning. *Trends Cogn. Sci. 2*(8), 275–281.

Crone, S. F., Hibon, M., & Nikolopoulos, K. (2011). Advances in forecasting with neural networks? Empirical evidence from the NN3 competition on time series prediction. *Int. J. Forecast.*, *27*(3), 635–660.

Dietterich, T. G. (2002). Machine learning for sequential data: A review. In *Proceedings of the Jt. IAPR Int. Work. Struct. Syntactic, Stat. Pattern Recognition* (pp. 15–30). Berlin: Springer-Verlag.

Domingos, P., & Hulten, G. (2000). Mining high-speed data streams. *Proceedings of the Sixth ACM SIGKDD Int. Conf. Knowl. Discov. Data Mining* (pp. 71–80). New York: ACM Press.

Durbin, J., & Koopman, S. J. (2012). *Time series analysis by state space methods* (2nd ed.). New York: Oxford University Press.

Fine, S., Singer, Y., & Tishby, N. (1998). The hierarchical hidden markov model: Analysis and applications. *Mach. Learn.*, *32*(1), 41–62.

Földiák, P. (2002). Sparse coding in the primate cortex. In M. A. Arbib (Ed.), *The handbook of brain theory and neural networks* (2nd ed.), (pp. 1064–1068). Cambridge, MA: MIT Press.

Gaber, M. M., Zaslavsky, A., & Krishnaswamy, S. (2005). Mining data streams. *ACM SIGMOD Rec.*, *34*(2), 18.

Gama, J. (2010). *Knowledge discovery from data streams*. Boca Raton, FL: Chapman and Hall/CRC.

Gavornik, J. P., & Bear M. F. (2014). Learned spatiotemporal sequence recognition and prediction in primary visual cortex. *Nat. Neurosci.*, *17*, 732–737.

Graves, A. (2012). *Supervised sequence labelling with recurrent neural networks*. New York: Springer.

Greff, K., Srivastava, R., Koutnik, J., Steunebrink, B. R., & Schmidhuber, J. (2015). *LSTM: A search space Odyssey.* arXiv.1503.04069

Hawkins, J., & Ahmad, S. (2016). Why neurons have thousands of synapses: A theory of sequence memory in neocortex. *Front. Neural Circuits*, *10*.

Hawkins, J., Ahmad, S., & Dubinsky, D. (2011). *Cortical learning algorithm and hierarchical temporal memory*. Numenta white paper. http://numenta.org/resources/HTM_CorticalLearningAlgorithms.pdf

Hebb, D. (1949). The organization of behavior: A neuropsychological theory. *Sci. Educ.*, *44*(1), 335.

Henaff, M., Szlam, A., & Lecun, Y. (2016). *Orthogonal RNNs and long-memory tasks*. arXiv.1602.06662

Hinton, G., Srivastava, N., Krizhevsky, A., Sutskever, I., & Salakhutdinov, R. (2012). *Improving neural networks by preventing co-adaptation of feature detectors.* arXiv.1207.0580

Hochreiter, S., & Schmidhuber, J. (1997). Long short-term memory. *Neural Comput.*, *9*(8), 1735–1780.

Huang, G.-B., Wang, D. H., & Lan, Y. (2011). Extreme learning machines: A survey. *Int. J. Mach. Learn. Cybern.*, *2*(2), 107–122.

Huang, G.-B., Zhu, Q.-Y., & Siew, C.-K. (2006). Extreme learning machine: Theory and applications. *Neurocomputing*, *70*, 489–501.

Hyndman, R. J., & Athanasopoulos, G. (2013). *Forecasting: Principles and practice*. OTexts, https://www.otexts.org/fpp.

Hyndman, R. J., & Khandakar, Y. (2008). Automatic time series forecasting: The forecast package for R. *J. Stat. Softw.*, *26*(3).

Igel, C., & Hüsken, M. (2003). Empirical evaluation of the improved Rprop learning algorithms. *Neurocomputing*, *50*, 105–123.

Jaeger, H. (2002). *Tutorial on training recurrent neural networks, covering BPPT, RTRL, EKF and the "echo state network" approach* (GMD Rep. 159. 48). Hanover: German National Research Center for Information Technology.

Jaeger, H., & Haas, H. (2004). Harnessing nonlinearity: Predicting chaotic systems and saving energy in wireless communication. *Science*, *304*(5667), 78–80.

Kanerva, P. (1988). *Sparse distributed memory*. Cambrige, MA: MIT Press.

Lavin, A., & Ahmad, S. (2015). Evaluating real-time anomaly detection algorithms: The Numenta anomaly benchmark. In *Proceedings of the 14th Int. Conf. Mach. Learn. Appl.* Piscataway, NJ: IEEE.

LeCun, Y., Bengio, Y., & Hinton, G. (2015). Deep learning. *Nature*, *521*(7553), 436–444.

Lee, M., Hwang, K., & Sung, W. (2014). Fault tolerance analysis of digital feedforward deep neural networks. In *Proceedings of the 2014 IEEE Int. Conf. Acoust. Speech Signal Processing*, (pp. 5031–5035). Piscataway, NJ: IEEE.

Liang, N.-Y., Huang, G.-B., Saratchandran, P., & Sundararajan, N. (2006). A fast and accurate online sequential learning algorithm for feedforward networks. *IEEE Trans. Neural Netw.*, *17*(6), 1411–1423.

Lipton, Z. C., Berkowitz, J., & Elkan, C. (2015). *A critical review of recurrent neural networks for sequence learning*. arXiv.1506.00019[cs.LG]

Lughofer, E., & Angelov, P. (2011). Handling drifts and shifts in on-line data streams with evolving fuzzy systems. *Appl. Soft Comput.*, *11*(2), 2057–2068.

Major, G., Larkum, M. E., & Schiller, J. (2013). Active properties of neocortical pyramidal neuron dendrites. *Annu. Rev. Neurosci.*, *36* 1–24.

Massey, P. V., & Bashir, Z. I. (2007). Long-term depression: Multiple forms and implications for brain function. *Trends Neurosci.*, *30*(4), 176–184.

Mauk, M. D., & Buonomano, D. V. (2004). The neural basis of temporal processing. *Annu. Rev. Neurosci.*, *27*, 307–340.

McFarland, J. M., Cui, Y., & Butts, D. A. (2013). Inferring nonlinear neuronal computation based on physiologically plausible inputs. *PLoS Comput. Biol.*, *9*(7), e1003143.

Mikolov, T., Chen, K., Corrado, G., & Dean, J. (2013). *Efficient estimation of word representations in vector space*. arXiv.1301.3781

Mnatzaganian, J., Fokoué, E., & Kudithipudi, D. (2016). *A mathematical formalization of hierarchical temporal memory's spatial pooler*. arXiv.1601.06116.

Moreira-Matias, L., Gama, J., Ferreira, M., Mendes-Moreira, J., & Damas, L. (2013). Predicting taxi–passenger demand using streaming data. *IEEE Trans. Intell. Transp. Syst.*, *14*(3), 1393–1402.

Mountcastle, V. B. (1997). The columnar organization of the neocortex. *Brain*, *120* (Pt. 4), 701–722.

Nikolić, D., Häusler, S., Singer, W., & Maass, W. (2009). Distributed fading memory for stimulus properties in the primary visual cortex. *PLoS Biol.*, *7*(12), e1000260.

Olshausen, B. A., & Field, D. J. (2004). Sparse coding of sensory inputs. *Curr. Opin. Neurobiol.*, *14*, 481–487.

Polsky, A., Mel, B. W., & Schiller, J. (2004). Computational subunits in thin dendrites of pyramidal cells. *Nat. Neurosci.*, *7*(6), 621–627.

Ponulak, F., & Kasiński, A. (2010). Supervised learning in spiking neural networks with ReSuMe: Sequence learning, classification, and spike shifting. *Neural Comput.*, *22*(2), 467–510.

Purdy, S. (2016). *Encoding data for HTM systems*. arXiv.1602.05925

Rabiner, L., & Juang, B. (1986). An introduction to hidden Markov models. *IEEE ASSP Mag.*, *3*(1), 4–16.

Rao, R. P., & Sejnowski, T. J. (2001). Predictive learning of temporal sequences in recurrent neocortical circuits. In *Proceedings of the Novartis Found. Symp.*, *239*, (pp. 208–229; discussion 229–240).

Sadato, N., Pascual-Leone, A., Grafman, J., Ibañez, V., Deiber, M. P., & Hallett, M. (1996). Activation of the primary visual cortex by Braille reading in blind subjects. *Nature*, *380*(6574), 526–528.

Sayed-Mouchaweh, M., & Lughofer, E. (2012). *Learning in non-stationary environments: Methods and applications*. New York: Springer.

Schaul, T., Bayer, J., Wierstra, D., Sun, Y., Felder, M., Sehnke, F., . . . Schmidhuber, J. (2010). PyBrain. *J. Mach. Learn. Res*. *11*, 743–746.

Schmidhuber, J. (2009). Simple algorithmic theory of subjective beauty, novelty, surprise, interestingness, attention, curiosity, creativity, art, science, music, jokes. *Journal of the Society of Instrument and Control Engineers*, *48*(1), 21–32.

Schmidhuber, J. (2014). Deep learning in neural networks: An overview. *Neural Networks*, *61*, 85–117.

Sejnowski, T., & Rosenberg, C. (1987). Parallel networks that learn to pronounce English text. *J. Complex Syst.*, *1*(1), 145–168.

Sharma, J., Angelucci, A., & Sur, M. (2000). Induction of visual orientation modules in auditory cortex. *Nature*, *404*(6780), 841–847.

Smith, S. L., Smith, I. T, Branco, T., & Häusser, M. (2013). Dendritic spikes enhance stimulus selectivity in cortical neurons in vivo. *Nature*, *503*(7474), 115–120.

Spruston, N. (2008). Pyramidal neurons: Dendritic structure and synaptic integration. *Nat. Rev. Neurosci.*, *9*(3), 206–221.

Sutskever, I., Vinyals, O., & Le, Q. V. (2014). Sequence to sequence learning with neural networks. In Z. Ghahramani, M. Welling, C. Cortes, N. D. Lawrence, & K. Q. Weinberger (Eds.), *Advances in neural information processing systems, 27* (pp. 3104–3112). Red Hook, NY: Curran.

Tchernev, E. B., Mulvaney, R. G., & Phatak, D. S. (2005). Investigating the fault tolerance of neural networks. *Neural Comput.*, *17*(7), 1646–1664.

Tran, A. H., Yanushkevich, S. N., Lyshevski, S. E., & Shmerko, V. P. (2011). Design of neuromorphic logic networks and fault-tolerant computing. In *Proceedings of the 2011 11th IEEE Int. Conf. Nanotechnology*, (pp. 457–462). Piscataway, NJ: IEEE.

Waibel, A., Hanazawa, T., Hinton, G., Shikano, K., & Lang, K. J. (1989). Phoneme recognition using time-delay neural networks. *IEEE Trans. Acoust.*, *37*(3), 328–339.

Wang, X., & Han, M. (2014). Online sequential extreme learning machine with kernels for nonstationary time series prediction. *Neurocomputing*, *145*, 90–97.

Williams, R. J., & Peng, J. (1990). An efficient gradient-based algorithm for on-line training of recurrent network trajectories. *Neural Comput.*, *2*(4), 490–501.

Williams, R. J., & Zipser, D. (1989). A learning algorithm for continually running fully recurrent neural networks. *Neural Comput.*, *1*(2), 270–280.

Xu, S., Jiang, W., Poo, M.-M., & Dan, Y. (2012). Activity recall in a visual cortical ensemble. *Nat. Neurosci.*, *15*(3), 449–455, S1–S2.

Zito, K., & Svoboda, K. (2002). Activity-dependent synaptogenesis in the adult Mammalian cortex. *Neuron*, *35*(6), 1015–1017.

Received December 10, 2015; accepted July 11, 2016.

This article has been cited by:

1. Valentin Puente, José Ángel Gregorio. 2019. CLASSIC: A cortex-inspired hardware accelerator. *Journal of Parallel and Distributed Computing* **134**, 140-152. [Crossref]
2. Tengyao Li, Buhong Wang, Fute Shang, Jiwei Tian, Kunrui Cao. 2019. Online sequential attack detection for ADS-B data based on hierarchical temporal memory. *Computers & Security* **87**, 101599. [Crossref]
3. Alexandre Payeur, Jean-Claude Béïque, Richard Naud. 2019. Classes of dendritic information processing. *Current Opinion in Neurobiology* **58**, 78-85. [Crossref]
4. Luong Ha Nguyen, James-A. Goulet. 2019. Real-time anomaly detection with Bayesian dynamic linear models. *Structural Control and Health Monitoring* **26**:9. . [Crossref]
5. K. P. Sridhar, S. Baskar, P. Mohamed Shakeel, V. R. Sarma Dhulipala. 2019. Developing brain abnormality recognize system using multi-objective pattern producing neural network. *Journal of Ambient Intelligence and Humanized Computing* **10**:8, 3287-3295. [Crossref]
6. Tien Van Nguyen, Khoa Van Pham, Kyeong-Sik Min. 2019. Hybrid Circuit of Memristor and Complementary Metal-Oxide-Semiconductor for Defect-Tolerant Spatial Pooling with Boost-Factor Adjustment. *Materials* **12**:13, 2122. [Crossref]
7. Dario Dematties, Silvio Rizzi, George K. Thiruvathukal, Alejandro Wainselboim, B. Silvano Zanutto. 2019. Phonetic acquisition in cortical dynamics, a computational approach. *PLOS ONE* **14**:6, e0217966. [Crossref]
8. Sergio Garcia-Vega, Xiao-Jun Zeng, John Keane. 2019. Learning from data streams using kernel least-mean-square with multiple kernel-sizes and adaptive step-size. *Neurocomputing* **339**, 105-115. [Crossref]
9. Jakob Struye, Steven Latré. 2019. Hierarchical temporal memory and recurrent neural networks for time series prediction: An empirical validation and reduction to multilayer perceptrons. *Neurocomputing* . [Crossref]
10. Olga Krestinskaya, Alex Pappachen James. AnalogHTM: Memristive Spatial Pooler Learning with Backpropagation 262-266. [Crossref]
11. Emily L Mackevicius, Andrew H Bahle, Alex H Williams, Shijie Gu, Natalia I Denisenko, Mark S Goldman, Michale S Fee. 2019. Unsupervised discovery of temporal sequences in high-dimensional datasets, with applications to neuroscience. *eLife* **8**. . [Crossref]
12. Meng Sun, Haopeng Chen. Heuristic Prefetching Caching Strategy to Enhance QoE in Edge Computing 438-445. [Crossref]
13. Shinichiro Naito, Masafumi Hagiwara. Hierarchical Temporal Memory Introducing Time Axis in Connection Segments 1364-1369. [Crossref]

14. Sotetsu Suzugamine, Takeru Aoki, Keiki Takadama, Hiroyuki Sato. A Study on a Cortical Learning Algorithm Dynamically Adjusting Columns and Cells 267-274. [Crossref]
15. Maria A. Rodriguez, Ramamohanarao Kotagiri, Rajkumar Buyya. 2018. Detecting performance anomalies in scientific workflows using hierarchical temporal memory. *Future Generation Computer Systems* **88**, 624-635. [Crossref]
16. Benedikt Feldotto, Florian Walter, Florian Röhrbein, Alois Knoll. 2018. Hebbian learning for online prediction, neural recall and classical conditioning of anthropomimetic robot arm motions. *Bioinspiration & Biomimetics* **13**:6, 066009. [Crossref]
17. Pablo A. Henríquez, Gonzalo A. Ruz. 2018. A non-iterative method for pruning hidden neurons in neural networks with random weights. *Applied Soft Computing* **70**, 1109-1121. [Crossref]
18. E.N. Osegi. 2018. Using the Hierarchical Temporal Memory Spatial Pooler for short-term forecasting of electrical load time series. *Applied Computing and Informatics* . [Crossref]
19. Marco Martinolli, Wulfram Gerstner, Aditya Gilra. 2018. Multi-Timescale Memory Dynamics Extend Task Repertoire in a Reinforcement Learning Network With Attention-Gated Memory. *Frontiers in Computational Neuroscience* **12**. . [Crossref]
20. Olga Krestinskaya, Timur Ibrayev, Alex Pappachen James. 2018. Hierarchical Temporal Memory Features with Memristor Logic Circuits for Pattern Recognition. *IEEE Transactions on Computer-Aided Design of Integrated Circuits and Systems* **37**:6, 1143-1156. [Crossref]
21. Yunfei Gu, Samiran Ganguly, Mircea R. Stan, Avik W. Ghosh. Hardware based spatio-temporal neural processing backend for imaging sensors: Towards a smart camera 32. [Crossref]
22. Chundong Wang, Zhentang Zhao, Liangyi Gong, Likun Zhu, Zheli Liu, Xiaochun Cheng. 2018. A Distributed Anomaly Detection System for In-Vehicle Network Using HTM. *IEEE Access* **6**, 9091-9098. [Crossref]
23. Peer Neubert, Subutai Ahmad, Peter Protzel. A Sequence-Based Neuronal Model for Mobile Robot Localization 117-130. [Crossref]
24. Sergio Garcia-Vega, Xiao-Jun Zeng, John Keane. 2018. Stock Price Prediction Using Kernel Adaptive Filtering Within a Stock Market Interdependence Approach. *SSRN Electronic Journal* . [Crossref]
25. Sergio Garcia-Vega, Xiao-Jun Zeng, John Keane. 2018. Learning from Data Streams Using Kernel Adaptive Filtering. *SSRN Electronic Journal* . [Crossref]
26. Timur Ibrayev, Olga Krestinskaya, Alex Pappachen James. Design and implication of a rule based weight sparsity module in HTM spatial pooler 274-277. [Crossref]

27. Yuwei Cui, Subutai Ahmad, Jeff Hawkins. 2017. The HTM Spatial Pooler—A Neocortical Algorithm for Online Sparse Distributed Coding. *Frontiers in Computational Neuroscience* **11**. . [Crossref]
28. Subutai Ahmad, Alexander Lavin, Scott Purdy, Zuha Agha. 2017. Unsupervised real-time anomaly detection for streaming data. *Neurocomputing* **262**, 134-147. [Crossref]
29. Dikio C. Idoniboyeobu, Biobele A. Wokoma, Emmanuel N. Osegi. Fault location prediction on double-circuit transmission lines based on the hierarchical temporal memory 1100-1105. [Crossref]
30. William Softky, Criscillia Benford. 2017. Sensory Metrics of Neuromechanical Trust. *Neural Computation* **29**:9, 2293-2351. [Abstract] [Full Text] [PDF] [PDF Plus]
31. Yan Pang, Haoguang Li. Short-term harmonic forecasting and evaluation affected by electrified railways on the power grid based on stack auto encoder neural network method 1071-1076. [Crossref]
32. William Softky, Criscillia Benford. Sensory Metrics of Neuromechanical Trust. *Neural Computation*, ahead of print1-59. [Abstract] [PDF] [PDF Plus]
33. James Mnatzaganian, Ernest Fokoué, Dhireesha Kudithipudi. 2017. A Mathematical Formalization of Hierarchical Temporal Memory's Spatial Pooler. *Frontiers in Robotics and AI* **3**. . [Crossref]